

## Transition metals and their carbides and nitrides: Trends in electronic and structural properties

Jeffrey C. Grossman, Ari Mizel, Michel Côté, Marvin L. Cohen, and Steven G. Louie

*Department of Physics, University of California at Berkeley, Berkeley, California 94720*

*and Materials Science Division, Lawrence Berkeley National Laboratory, Berkeley, California 94720*

(Received 31 August 1998)

A study of the structural and electronic properties of selected transition metals and their carbides and nitrides is presented. We focus on assessing trends of possible importance for understanding their hardness. Lattice constants, bulk moduli ( $B_o$ ), and charge densities are calculated using the local density approximation with a pseudopotential plane wave approach. An fcc lattice is employed for the transition metal elements in order to make comparisons and study trends relateable to their carbides and nitrides. Our results show that both increasing the number of valence  $d$  electrons and the presence of  $f$  electrons in the core lead to larger ( $B_o$ ). Charge density plots and histograms enable us to explain the nature of the charge distribution in the interstitial region for the different compounds considered. In addition, we include the heavier elements seaborgium, bohrium, and hasnium in order to test further trends. Surprisingly, the calculated  $B_o$  for Hs is comparable to that of diamond. [S0163-1829(99)03630-9]

Advances in *ab initio* electronic structure computation techniques have made possible the calculation of crystal structures and elastic properties for many materials to within 2–5% of experimental results. Such advances in accurate theoretical modelling have created new opportunities for studying hard materials. For example, theoretical predictions of hard structures<sup>1,2</sup> have led to a multitude of recent experimental efforts<sup>3</sup> to synthesize superhard materials. Here, we study transition metals and transition metal carbides and nitrides, which are known for their hardness and industrial usefulness. There is a large body of literature concerning these materials in their experimental lattice structures.<sup>4–8</sup> However, state of the art first principles computational modelling now permits the comparison of electronic and elastic properties of different elements and compounds all within the same crystal structure.<sup>9–13</sup> In this way, one can explore trends in the structural and electronic properties to identify qualities of these materials which may be relevant for hardness. In this work, we focus attention on the bulk moduli of these solids, which, although not always directly correlated with hardness, provide a clearly defined theoretical basis for the investigation of trends.

The following elements are included in this study. Beginning with Ti, we proceed across the Periodic Table to V and Cr, continue down to Mo and W, and then across again to Re and Os. This set of elements is chosen to (i) study the impact on  $B_o$  of increasing the principle quantum number of the valence electrons, (ii) systematically explore the effect on  $B_o$  of increasing the number of valence  $d$ -electrons; and (iii) include a wide variety of hard solids which have proven useful in technological applications. This collection of elements should be sufficiently rich to illustrate some principle trends in hardness-related properties.

In addition, we have performed local density approximation (LDA) calculations on the heavy elements seaborgium (Sg<sup>106</sup>), bohrium (Bh<sup>107</sup>), and hasnium (Hs<sup>108</sup>) in order to test further some of the observed trends. Of course, it is

impractical to contemplate the actual use of these heavy elements in constructing hard materials. (Although the reader may find it interesting to discover that seaborgium, in particular, is sufficiently stable to permit chemical investigation.<sup>14</sup>) However, because Sg, Bh, and Hs are isoelectronic in the valence with the stable elements W, Re, and Os, these heavy elements can serve a useful purpose in testing trends.

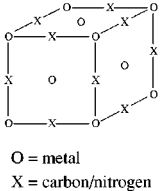
A plane wave pseudopotential total-energy scheme<sup>15,16</sup> is used to calculate the electronic structure and structural parameters and to compute total energies of different phases for all these metals and compounds. We employ the local density approximation<sup>17</sup> and use the Ceperley-Alder interpolation formula<sup>18</sup> for the exchange-correlation energy. *Ab initio* pseudopotentials are generated using the method of Troullier and Martins<sup>19</sup> and include semirelativistic corrections. Spin-orbit coupling is excluded from these calculations in order to eliminate additional variables to allow a focus on the simplest underlying trends.

For each calculation, irreducible  $k$ -points are generated according to the Monkhorst-Pack scheme.<sup>20</sup> Convergence is achieved with a range of 10–28  $k$ -points in the irreducible part of the Brillouin zone, depending on the compound. The different compounds require cutoff energies of 90–120 Ry to ensure convergence in the total energy to less than 1 mRy per atom. For all crystals considered here, we compute lattice constants and bulk moduli by fitting the energy versus volume curve to the Murnigan equation of state.<sup>21</sup>

Note that LDA calculated bulk moduli typically agree with those of experiment to within about 2–5%. This LDA error is relevant when making comparisons among the different solids considered in the present study; in particular, differences of  $\approx 5\%$  in  $B_o$  should not be viewed as significant.

Some of the transition metal carbides and nitrides considered here are observed experimentally to crystallize in the rocksalt structure (TiC, TiN, VC, VN, and CrN), while others are known to crystallize in a hexagonal structure (MoC,

Ti	119 267 304	V	191 321 338	Cr	264 351 361	pure element carbide nitride			
				Mo	261 353 354				
				W	315 396 394		Re	399 404 396	Os
				Sg	289 408 411	Bh	389 398 399	Hs	450 392 368

O = metal  
X = carbon/nitrogen

FIG. 1. Calculated bulk moduli (GPa) for selected transition metals and transition metal carbides and nitrides. As shown, the number in the first line corresponds to  $B_o$  of the pure element and the second and third lines correspond to  $B_o$  of the carbide and nitride of that element, respectively. Positions of the atoms in the lattice are also shown.

WC, WN, and OsC). Crystal structures of the remaining carbide and nitride compounds are not determined experimentally. To facilitate comparison of charge densities and other electronic properties, we choose the rocksalt structure for all carbides and nitrides appearing in this study. Such an approximation implies that quantitative results cannot be inferred from the present calculations. However, our intent here is specifically to make comparisons among hypothetical, possibly non-physical systems in order to eliminate as many variables as possible so as to isolate and study particular trends.<sup>9-13</sup> The positions of the transition metal atoms within the rocksalt structure form an fcc lattice (see inset of Fig. 1).

Most of the transition metal elements considered in the present study are found experimentally to crystallize in the bcc or hcp structure. However, the use of *ab initio* computational methods allows us to investigate the fcc structure of the pure elements, which permits direct comparisons of the charge densities and lattice constants with those of their carbides and nitrides. A similar approach was used, for example, to examine various contributions to the enthalpies of formation of 24 different transition metals and their carbides and nitrides.<sup>22</sup> Even though fcc is not their ground state, it turns out that our computed bulk moduli are close to experimentally measured values.

The equilibrium lattice constants corresponding to each of these solids are shown in Table I. Note that the trend in lattice constants follows that of the atomic radii: the values increase as one proceeds leftward and downward on the Periodic Table. Our results for the pure elements are in very good agreement with those of Ref. 22 and close to experimental values.

In Fig. 1, we present our calculated bulk moduli for all the solids appearing in this work. (Note that the computed bulk modulus for these challenging *d*-level systems appears to depend on the computational method employed.<sup>9,10</sup>) For the pure elements, we note first the dramatic increase in  $B_o$  in going from Ti to Cr. Proceeding downward, we find that Cr and Mo have the same  $B_o$  to within the accuracy of our

TABLE I. Equilibrium lattice constants ( $\text{\AA}$ ) computed within LDA for the fcc transition metals and their carbide and nitride compounds.

	Element	Carbide	Nitride
Ti	4.12	4.38	4.32
V	3.86	4.22	4.19
Cr	3.62	4.10	4.09
Mo	4.00	4.42	4.41
W	4.01	4.38	4.36
Re	3.88	4.33	4.31
Os	3.83	4.33	4.32
Sg	4.09	4.38	4.32
Bh	4.02	4.43	4.41
Hs	3.95	4.38	4.37

calculations. However, moving down one more row to W results in a substantial increase in  $B_o$ . Traversing further across the table to Re and Os yields another increase in  $B_o$ .

The heavy elements, Sg, Bh, and Hs, exhibit the same pattern as W, Re, and Os: the bulk modulus increases with the number of valence *d* electrons. However, Sg is somewhat anomalous in that it has a smaller  $B_o$  than W even though it lies below W in the periodic table.

In addition to pure fcc transition metals, Fig. 1 includes our computed bulk moduli for rocksalt carbide and nitride compounds. Experimentally, these compounds generally possess larger bulk moduli than the corresponding pure elements. We find a similar result in our computations. For Ti through W, we find that  $B_o$  for the carbides and nitrides follows patterns broadly similar to those found in the pure elements. These patterns are often disobeyed, however, for solids involving elements heavier than W.

Perhaps the most obvious trend in the pure elements is that  $B_o$  increases dramatically as the number of valence electrons increases. This result may indicate that the additional electrons contribute charge to the bonds of the solid and strengthen them. In order to test this effect, we compute valence charge densities for Ti, Cr, W, and Os, as shown in Fig. 2. In Ti [Fig. 2(a)], the charge is rather localized near the core—i.e., there is a large, flat region between atoms. In Cr [Fig. 2(b)], flat interstitial region is reduced in size—i.e., there is more valence charge in the between atoms due to the extra two electrons compared with Ti.

If we now compare with the charge densities of W [Fig. 2(c)] and Os [Fig. 2(d)], more dramatic differences are observed. For example, W is isoelectronic with Cr; however, the core region in W is much larger, pushing the valence charge into the interstitial regions. Thus, even though the maximum charge density in Cr is larger than in W, there is more charge on the bonds in W, leading to the larger bulk modulus. Two more electrons are added to get from W to Os, and they enhance the charge density throughout the plot. Osmium has the most charge in the interstitial bonding region and it also has the largest  $B_o$  of the four elements in Fig. 2.

In order to assess further the nature of the charge distribution, we have also plotted a histogram of these charge densities. Such a plot quantifies the extent to which the charge is distributed homogeneously in the interstitial region

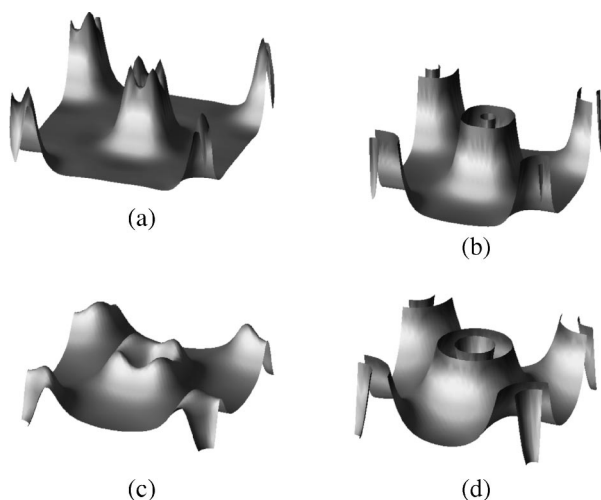


FIG. 2. Valence charge density plots for (a) Ti, (b) Cr, (c) W, and (d) Os in the fcc crystal structure in the (1,0,0) plane. The peaks and troughs in the core region are due to the pseudopotentials and should be ignored for the purposes of this study.

or inhomogeneously into bonds. A single, sharp peak in the histogram at a given density indicates a delocalized, uniform charge distribution. A broader spectrum of densities indicates that the interstitial region is not uniformly charged and there are regions of high density bonding.

In Fig. 3, the distribution of densities  $f(\rho)$  is plotted as a

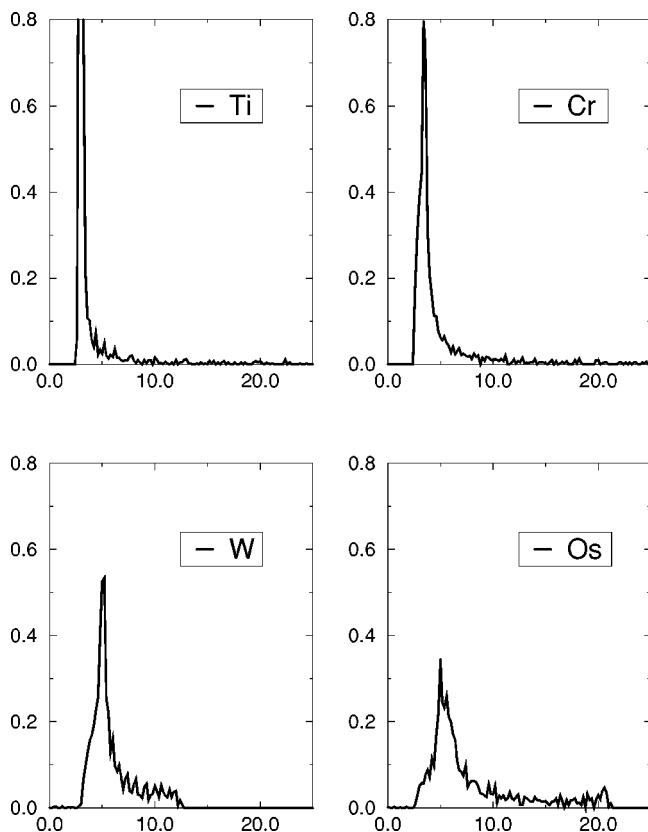


FIG. 3. Histogram of the valence charge densities of Ti, Cr, W, and Os. In each plot, the  $x$  axis corresponds to the charge density (electrons/bohr<sup>3</sup>) and the  $y$  axis corresponds to the distribution of densities as a function of charge density.

function of the charge density for the same four elements. Normalization is such that the first moment of each graph corresponds to the total number of valence electrons (4, 6, 6, and 8 for Ti, Cr, W, and Os, respectively). Thus,  $\int f(\rho)\rho d\rho = \text{no. electrons/unit cell}$ . Note that for Ti and Cr there is one large peak which quickly diminishes to small fluctuations near zero as the charge density increases. This result indicates that in both cases the density of charge in the system has essentially a constant value outside of the cores. The small fluctuations at higher densities correspond to the localized charge near the cores. In Cr, the peak is shifted and slightly broader with respect to Ti, indicating the larger average value of the density in Cr. Thus, it is clear that Ti and Cr have a relatively homogeneous charge distribution in the interstitial regions, which surrounds the localized  $d$ -states of the atoms.

In the case of W, the picture changes dramatically. A comparison with Cr which has the same number of valence electrons reveals that W has a much broader histogram of charge densities as well as a shift of the peak to higher density. The charge in W therefore is less like a free electron gas and more directionally bonded. The fluctuations out to higher densities are significantly larger than in Cr, illustrating this effect. In Os, the charge is even more localized on the bonds and the extra electrons with respect to W contribute to strong directional bonding.

Another observation is that sixth row transition elements (i.e., those with  $5d$  electrons) have substantially larger bulk moduli than the elements in the 4th and 5th rows. Indeed, while the bulk moduli of Cr and Mo are essentially the same, the bulk modulus of W is calculated to be  $\approx 50$  GPa higher. This increase may be due to the presence of  $f$ -electrons in the cores of the sixth row atoms. These  $f$ -electrons push out the spatial extent of the valence  $d$ -orbitals which allows them to make stronger directional bonds.

In comparing Cr to Mo, the bulk modulus  $B_o$  does not change very much, while the lattice constant increases significantly. This stands as a counterexample to the general notion that the bulk modulus and lattice constant are inversely related. The difference in lattice constant can most likely be traced to the isolated atoms: the spatial extent of the  $4d$  orbitals in a Mo atom is greater than the spatial extent of the  $3d$  orbitals in a Cr atom.

The presence of C or N in the transition metal compounds introduces a different kind of bonding involving hybridized  $p$ - $d$  orbitals. As a result, one would not *a priori* expect a connection between  $B_o$  for an element and  $B_o$  for the corresponding carbide and nitride compounds. It is therefore interesting to note that the bulk moduli are in fact strongly correlated: in general, if  $B_o$  is large for an element, it will be large for the corresponding carbide or nitride. In addition, despite the qualitative change in the bonding, many of the trends that hold for the pure elements are echoed in the carbides and nitrides.

As mentioned, in the case of Ti the charge density plot indicates relatively homogeneous charge distribution in the interstitial region. The addition of C or N seems to permit directional bonds to form due to the hybridization of the  $p$  and  $d$  orbitals. This effect significantly increases the strength of the structure. In the case of W, Re, and Os, directional bonding is already present in the pure elements; the addition

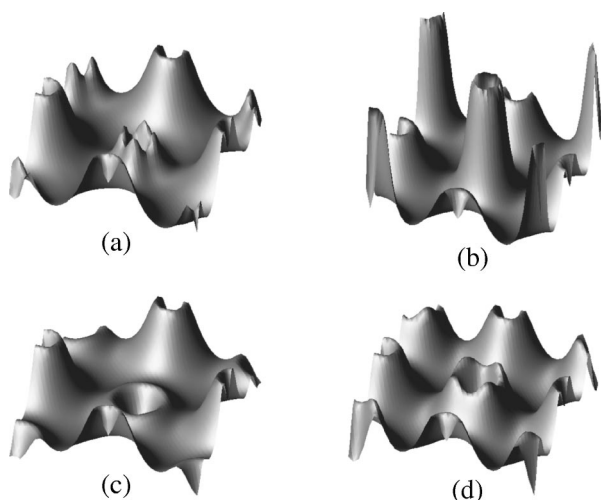


FIG. 4. Valence charge density plots for (a) TiC, (b) CrC, (c) WC, and (d) OsC in the fcc crystal structure in the (1,0,0) plane. Metal atoms occupy the same positions as in Fig. 2, in the center and corners of each plot.

of C or N changes these directional bonds from metal-metal to metal-carbon or metal-nitrogen. Thus, the presence of C or N causes a less dramatic increase in  $B_o$  for W compared with Ti. Furthermore, in the carbides and nitrides the saturation of bonding states appears to be reached at W or Re, whereas for OsC and OsN the bulk moduli are actually lower than pure Os. This result indicates that antibonding states are starting to be occupied in the Os carbides and nitrides.

We test this picture by plotting in Fig. 4 the valence charge densities for the carbides: TiC, CrC, WC, and OsC. Note that directional bonds are indeed visible between the metal and carbon atoms. It is these new bonds that increase the bulk moduli for Ti, Cr, and W when compared to the pure elements because the charge distribution in the pure metals is much more like a free electron gas. In the case of Os, on the other hand, strong directional bonds are formed for the pure element, and no advantage is gained by the addition of C. In Fig. 5 we again quantify these effects by plotting a histogram of charge densities. In all of the carbides there is a much broader distribution of densities than in the corresponding pure metals, indicating the presence of directional bonds (i.e., the charge density varies substantially over the unit cell).

One clear difference between the pure elements and their carbides or nitrides is the fact that C or N can equalize the computed bulk moduli across the Period Table. For example, ReC and ReN have essentially the same  $B_o$  as WC and WN even though the  $B_o$  of pure Re is 85 GPa larger than that of pure W. Os has an even higher  $B_o$  than Re; however, OsC and OsN have lower  $B_o$  than Os or than ReC and ReN. Thus, the addition of C and N appears to decrease the number of  $d$ -electrons needed to be present before the  $B_o$  has reached a maximum for a given row. The exact same trend is observed in the row beneath: Bh is higher than Sg and Hs is higher than Bh, but while SgC and SgN are significantly larger than Sg, BhC and BhN are roughly the same as Bh, and HsC and HsN are significantly weaker than Hs.

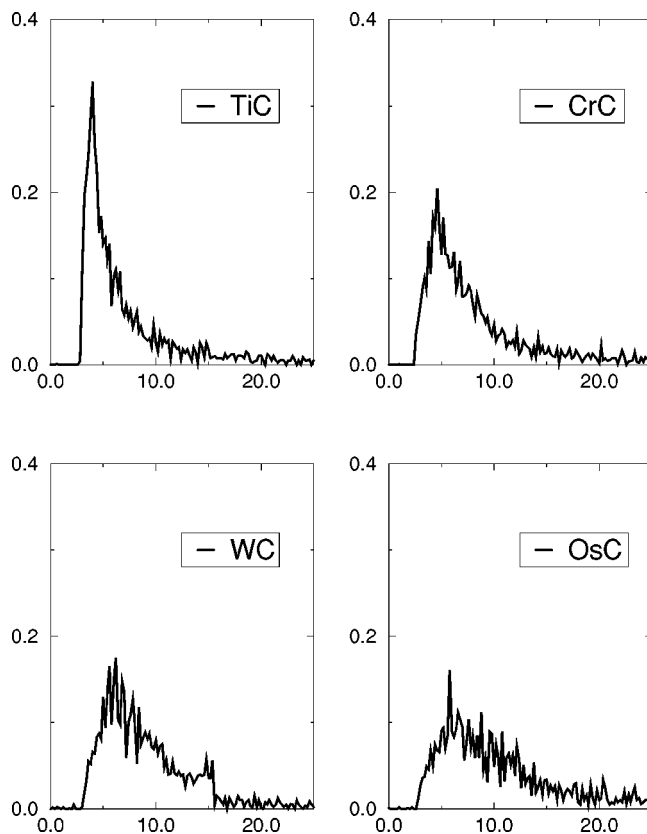


FIG. 5. Histogram of the valence charge densities of TiC, CrC, WC, and OsC. In each plot, the  $x$  axis corresponds to the charge density (electrons/bohr<sup>3</sup>) and the  $y$  axis corresponds to the distribution of densities as a function of charge density.

In summary, we have carried out a series of calculations of bulk moduli for transition metals, transition metal carbides, and nitrides. Such a systematic consideration of elements may help to identify patterns of structural and electronic properties. We show that the addition of valence electrons in going across the periodic table from Ti to Cr and W to Os significantly increases computed  $B_o$ . Furthermore, it is demonstrated that in moving down the periodic table one observes changes in the nature of the charge distribution in the interstitial region from homogeneous to stronger, more directional bonding. Our calculations also illustrate the effects of adding carbon or nitrogen to the transition metals. For the elements which have a homogenous interstitial charge distribution, a kind of directional bonding is introduced which dramatically increases  $B_o$ . In addition, the peak in  $B_o$  as a function of column in the Periodic Table is shifted to the left with respect to the pure elements. Finally, our calculations of the heavier elements Sg, Bh, and Hs provide further comparisons and illustrate the trends more clearly.

This work was supported by National Science Foundation Grant No. DMR-9520554, and the Director, Office of Energy Research, Office of Basic Energy Services, Materials Sciences Division of the U.S. Department of Energy under Contract No. DE-AC03-76SF00098. A.M. acknowledges the support of the National Science Foundation.

- <sup>1</sup>M. L. Cohen, Phys. Rev. B **32**, 7988 (1985).
- <sup>2</sup>A. Y. Liu and M. L. Cohen, Science **245**, 841 (1989).
- <sup>3</sup>For example, J. V. Badding and D. C. Nesting, Chem. Mater. **8**, 535 (1996).
- <sup>4</sup>J. P. Perdew, H. Q. Tran, and E. D. Smith, Phys. Rev. B **42**, 11627 (1990).
- <sup>5</sup>H. B. Shore and J. H. Rose, Phys. Rev. Lett. **66**, 2519 (1991).
- <sup>6</sup>J. H. Rose and H. B. Shore, Phys. Rev. B **49**, 11588 (1994).
- <sup>7</sup>K. F. Wojciechowski, Phys. Rev. B **53**, 961 (1996).
- <sup>8</sup>Y. Makino, J. Alloys Compd. **242**, 122 (1996).
- <sup>9</sup>H. Shimizu, M. Shirai, and N. Suzuki, J. Phys. Soc. Jpn. **66**, 3147 (1997).
- <sup>10</sup>V. P. Zhukov, V. A. Gubanov, O. Jepsen, N. E. Christensen, and O. K. Andersen, J. Phys. Chem. Solids **49**, 841 (1988).
- <sup>11</sup>A. Fernández Guillermet, J. Häglund, and G. Grimvall, Phys. Rev. B **48**, 11673 (1993).
- <sup>12</sup>A. Fernández Guillermet, J. Häglund, and G. Grimvall, Phys. Rev. B **45**, 11557 (1992).
- <sup>13</sup>J. Häglund, G. Grimvall, and A. Fernández Guillermet, Phys. Rev. B **43**, 14400 (1991).
- <sup>14</sup>M. Schadel *et al.*, Nature (London) **388**, 6637 (1997).
- <sup>15</sup>J. Ihm, A. Zunger, and M. L. Cohen, J. Phys. C **12**, 4409 (1979).
- <sup>16</sup>M. L. Cohen, Phys. Scr. **T1**, 5 (1982).
- <sup>17</sup>W. Kohn and L. J. Sham, Phys. Rev. **140**, A1133 (1965).
- <sup>18</sup>D. M. Ceperley and B. J. Alder, Phys. Rev. Lett. **45**, 566 (1980).
- <sup>19</sup>J. L. Martins, N. Troullier, and S.-H. Wei, Phys. Rev. B **43**, 2213 (1991).
- <sup>20</sup>H. J. Monkhorst and J. D. Pack, Phys. Rev. B **13**, 5188 (1976).
- <sup>21</sup>F. D. Murnaghan, Proc. Natl. Acad. Sci. USA **30**, 244 (1944).
- <sup>22</sup>J. Häglund, A. Fernández Guillermet, G. Grimvall, and M. Körling, Phys. Rev. B **48**, 11685 (1993).